RESEARCH ARTICLE

Higher Validity, Lower Radiation: A New Ictal Single-Photon Emission Computed Tomography Framework

Felix Bitzer, BSc,[1,2] Lennart Walger, MSc,[1,2] Tobias Bauer, MD, BSc,[1,2] Freya Schulte,[1,2] Florian C. Gaertner, MD,[3] Matthias Schmitz,[1,2] Martin Schidlowski, PhD,[2] Randi von Wrede, MD,[2] Attila Rácz, MD,[2] Tobias Baumgartner, MD,[2] Vadym Gnatkovsky, MD,[2] Daniel Paech, MD,[1] Valeri Borger, MD,[4] Hartmut Vatter, MD,[4] Bernd Weber, MD,[5] Dominik L. Michels, PhD,[6] Tony Stöcker, PhD,[7] Markus Essler, MD,[3] Josemir W. Sander, MD, PhD,[8,9,10] Alexander Radbruch, MD, JD,[1] Rainer Surges, MD, MHBA,[2] and Theodor Rüber, MD[1,2]

Objective: To assess whether arterial spin labeling perfusion images of healthy controls can enhance ictal single-photon emission computed tomography analysis and whether the acquisition of the interictal image can be omitted.
Methods: We developed 2 pipelines: The first uses ictal and interictal images and compares these to single-photon emission computed tomography and arterial spin labeling of healthy controls. The second pipeline uses only the ictal image and the analogous healthy controls. Both pipelines were compared to the gold standard analysis and evaluated on data of individuals with epilepsy who underwent ictal single-photon emission computed tomography imaging during presurgical evaluation between 2010 and 2022. Fifty healthy controls prospectively underwent arterial spin labeling imaging. The correspondence between the detected hyperperfusion and the postoperative resection cavity or the presumably affected lobe was assessed using Dice score and mean Euclidean distance. Additionally, the outcomes of the pipelines were automatically assigned to 1 of 5 concordance categories.
Results: Inclusion criteria were met by 43 individuals who underwent epilepsy surgery and by 73 non-surgical individuals with epilepsy. Compared to the gold standard analysis, both pipelines resulted in significantly higher Dice scores and lower mean distances ($p < 0.05$). The combination of both provided localizing results in 85/116 cases, compared to 54/116 generated by the current gold standard analysis and the ictal image alone produced localizing results in 60/116 (52%) cases.
Interpretation: We propose a new ictal single-photon emission computed tomography protocol; it finds relevantly more ictal hyperperfusion, and halves the radiation dose in about half of the individuals.

ANN NEUROL 2024;96:1160–1173

View this article online at wileyonlinelibrary.com. DOI: 10.1002/ana.27061

Received Aug 8, 2023, and in revised form Jul 30, 2024. Accepted for publication Aug 5, 2024.

Address correspondence to Theodor Rüber, Department of Neuroradiology, University Hospital Bonn, Venusberg-Campus 1, 53127 Bonn, Germany. E-mail: theodor.rueber@ukbonn.de

From the [1]Department of Neuroradiology, University Hospital Bonn, Bonn, Germany; [2]Department of Epileptology, University Hospital Bonn, Bonn, Germany; [3]Department of Nuclear Medicine, University Hospital Bonn, Bonn, Germany; [4]Department of Neurosurgery, University Hospital Bonn, Bonn, Germany; [5]Institute of Experimental Epileptology and Cognition Research, University Hospital Bonn, Bonn, Germany; [6]Department of Computer Science, Technische Universität Darmstadt, Darmstadt, Germany; [7]MR Physics, German Center for Neurodegenerative Diseases (DZNE), Bonn, Germany; [8]Department of Clinical & Experimental Epilepsy, UCL Queen Square Institute of Neurology, London, UK; [9]Chalfont Centre for Epilepsy, Chalfont St Peter, UK; and [10]Department of Neurology, West China Hospital, Sichuan University, Chengdu, China

Additional supporting information can be found in the online version of this article.

One-third of individuals with epilepsy do not achieve seizure freedom with anti-seizure medication. For these individuals, epilepsy surgery can provide seizure freedom or reduction.[1] Ictal single-photon emission computed tomography (SPECT) is an advanced diagnostic modality employed in the presurgical work-up to detect the seizure onset zone.[2] Ictal SPECT leverages the property of certain radioactive tracers to accumulate in cerebral tissue linearly to regional perfusion[3] to visualize ictal hyperperfusion of the epileptogenic zone.[4] State-of-the-art post-processing methods, such as ictal-interictal SPECT Analysis by SPM (ISAS),[5] statistically compare the difference between the ictal image and an additional interictal image with scan-to-scan variation of healthy controls to identify areas of significant ictal hyperperfusion.[5–7] In this study we focus on 3 previously understudied areas of ictal SPECT.

First, many metrics employed to quantitatively assess the utility of analyses in the medical imaging field have not been applied to ictal SPECT imaging[8] including the average Euclidean distance between the ground truth and the prediction of analysis or the Dice score, which measures the spatial overlap between ground truth and prediction. We aimed to quantitatively compare the hyperperfusion detected by ISAS (ie, the prediction) with the resection cavity in surgical and the lobe containing the presumed seizure onset zone (pSOZ) in non-surgical individuals with epilepsy (ie, the ground truth) to determine the Dice score and mean Euclidean distance.

Second, we aimed to increase the power of ictal SPECT analysis by increasing the number of healthy controls to which ictal SPECT scans are compared. Current state-of-the-art pipelines, such as ISAS,[5] compare the ictal-interictal difference to the scan-to-scan variations of 14 openly available SPECT healthy controls, using a voxel-wise 2-sample *t*-test followed by thresholding via random field theory.[9] Whilst non-parametric permutation tests have become increasingly popular, as they have been shown to produce fewer false positive clusters,[10,11] there are no reports on their use in ictal SPECT imaging, and permutation tests with only 14 healthy controls provide highly discrete results lacking statistical power. Since acquiring SPECT images of healthy controls cannot be ethically justified due to the high radiation exposure, we acquired perfusion images of healthy controls using arterial spin labeling (ASL). This MRI perfusion technique uses blood water molecules as an endogenous tracer and produces reliable and reproducible data.[12–14] Building on this, we developed and evaluated an ictal-interictal SPECT post-processing analysis (IISASL) which combines SPECT controls with ASL controls.

Third, we planned to develop and evaluate a second post-processing pipeline, named ictal SPECT-ASL (ISASL), which uses solely ictal SPECT images, and compares these to SPECT and ASL controls, thereby halving the radiation exposure.

We hypothesized that expanding the control cohort with ASL images and implementing a permutation-based statistical test can increase the power of ictal SPECT analysis compared to a conventional ISAS analysis and that for many individuals with epilepsy, the ictal image suffices. We tested our hypotheses by developing the IISASL and the ISASL pipelines and validating them quantitatively and qualitatively. A schematic overview of the study design is shown in Figure 1.

Methods

Study Group

The inclusion criterion for individuals with epilepsy was SPECT imaging as part of the presurgical evaluation at the Department of Epileptology of the University Hospital in Bonn between 2010 and 2022. The cohort was subdivided depending on whether surgery was performed or not. Surgical outcome was categorized by Engel outcomes at the last follow-up, as extracted from the records.[15] Two ASL scans of 50 healthy controls (mean age: 26.6 ± 5.3 years; 26 female [54%]) were obtained on 2 separate days. Inclusion criteria for healthy controls were no history of neurological disease, age above 18 years, and no contraindication for MRI. All subjects provided written informed consent and the study was approved by the institutional review board of the University Hospital Bonn.

SPECT Imaging

All SPECT images were acquired at the Department of Nuclear Medicine of the University Hospital Bonn using an IRIX 3 head gamma camera (Philips Healthcare, Hamburg, Germany). Acquisition parameters can be found in the supplement (S1). SPECT images of 14 healthy controls were downloaded from the publicly available dataset (http://spect.yale.edu).[14]

ASL and Structural MRI

ASL images of healthy controls were acquired with a 3 Tesla MRI scanner (Siemens Healthineers, Erlangen, Germany) equipped with a 32-channel head coil. The in-house developed pseudo-continuous ASL (pCASL) sequence uses a 3D-GRASE readout and a 7-block Hadamard encoding.[14] Voxel-wise cerebral blood flow (CBF) calculations were obtained with the FMRIB software library (FSL) Bayesian Inference for Arterial Spin Labeling MRI (BASIL) toolkit and based on the general kinetic model and a variational Bayes approach.[16,17] A structural MRI volume was needed for co-registration and normalization of SPECT data. Structural 3D-T1 of

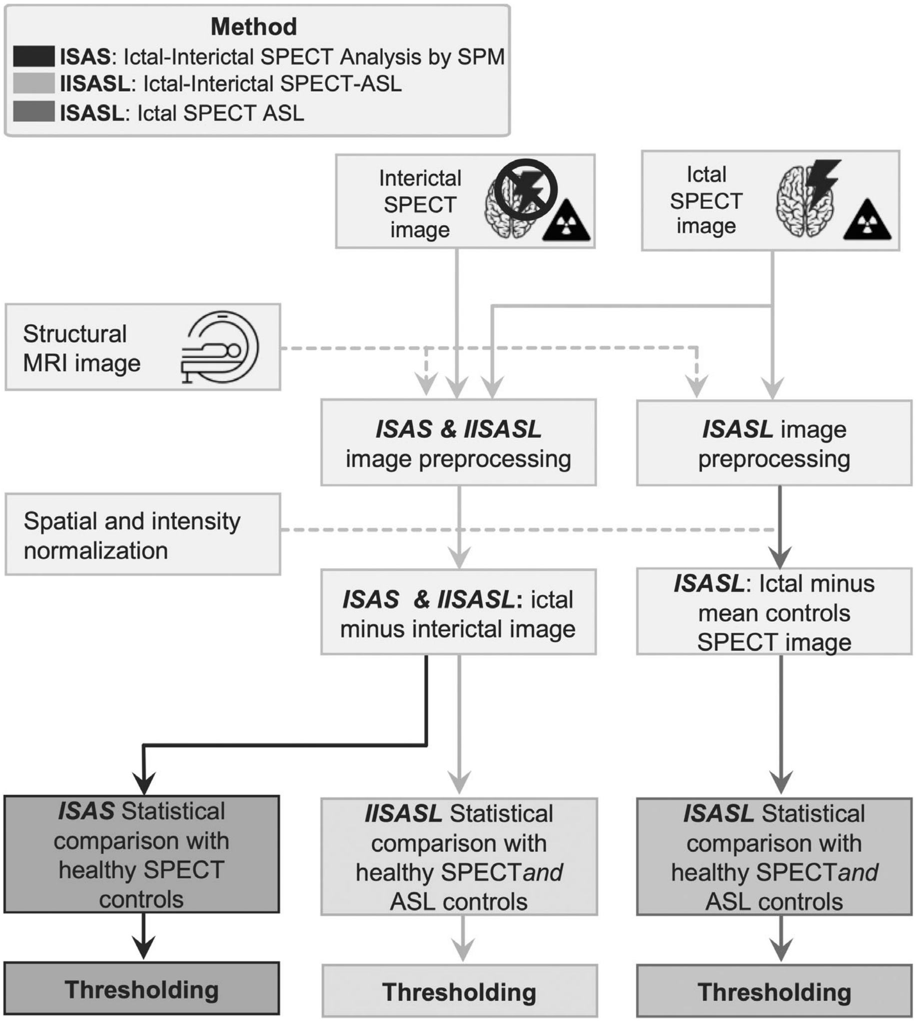

FIGURE 1: Schematic overview of the crucial steps of the ictal SPECT post-processing pipelines. ASL, arterial spin labeling; ISAS, interictal SPECT analysis by SPM; IISASL, ictal-interictal SPECT-ASL; ISASL, ictal SPECT-ASL.

individuals with epilepsy were also acquired on this scanner or in the department of neuroradiology at 3 T field strength.

Group Tests between SPECT and ASL Scan-to-Scan Differences

To rule out significant systematic differences between the SPECT and ASL histogram-matched scan-to-scan difference images of healthy controls, a voxel-wise 2-sample unpaired *t*-test with permutation-based non-parametric testing with 10,000 repetitions and FWE correction for multiple comparisons using threshold-free cluster enhancement (TFCE) was performed.[18]

Preprocessing of ISAS

To compare IISASL and ISASL to the conventional ISAS pipeline, we processed all individuals with epilepsy using the BioImage Suite Biswebnode implementation of ISAS[19] and choosing linear registration. Family-wise error (FWE) correction (with a threshold of $p < 0.05$) of the outputted t-score images in the native space of individuals with epilepsy was performed using random field theory with *FSL*.[20]

Preprocessing of IISASL and ISASL

Details are provided in the supplement (Table S2). Surface reconstruction of the structural MRI images was performed with *FastSurfer* (https://deep-mi.org/research/fastsurfer/),[21] and ictal and interictal SPECT images were registered to the individual structural images using *FreeSurfer* (version 6.0, https://surfer.nmr.mgh.harvard.edu/).[22] The anatomical image was spatially normalized to the MNI-152 standard space using *FSL* FNIRT.[20]

IISASL. Similar to ISAS, IISASL compares the ictal-interictal difference to the scan-to-scan differences of healthy controls to identify ictal hyperperfusion but uses a larger control cohort of both 50 ASL and 14 SPECT healthy controls. The ictal and interictal SPECT images of individuals with epilepsy were spatially, and intensity-normalized to the ASL template.[23] The individual ictal-interictal difference was smoothed and compared to the scan-to-scan variations of the SPECT and ASL controls using a voxel-wise 2-sample t-test with non-parametric testing applying extensive ($n = 64$) permutations, FWE correction for multiple comparisons, and TFCE.[18] To eliminate the scan-order bias of the healthy controls, the absolute values of the scan-to-scan differences between healthy controls and individuals with epilepsy were compared.

ISASL. The ISASL pipeline is equivalent to IISASL; however, instead of calculating ictal-interictal differences, the ictal difference to the mean SPECT image of healthy controls is calculated. The difference to the respective mean image was computed for each ASL and SPECT healthy controls and compared to the ictal-mean difference of the individuals with epilepsy by means of a voxel-wise 2-sample t-test with permutation-based non-parametric testing as in the IISASL pipeline.

Evaluation

Ground Truth. To evaluate the outcome of each pipeline (IISASL, ISASL, and ISAS) quantitative and qualitatively we first established a ground truth for each individual. The ground truth was defined by 2 types of masks depending on whether the individual underwent surgery: (1) In surgical individuals, a *resection mask* was defined. (2) In non-surgical individuals, the lobe containing the pSOZ was defined as *lobe mask*. Whilst analyses with the *resection masks* could only be performed for individuals who underwent surgery, analyses *lobe masks* were performed for both surgical and non-surgical individuals for consistency and to avoid bias.

(1) The *resection masks* were manually defined on post-surgical MRI using FSL.[20] The amygdala and hippocampus were defined as the ground truth for individuals without post-surgical MRIs who underwent amygdalohippocampectomy[24] For other surgical individuals without post-surgical MRI, masks were manually outlined based on the precise anatomical description of the planned surgical resection.

(2) *Lobe masks* included the temporal, frontal, occipital, parietal lobes, the insula, or the cingulate gyrus. The masks were based on the GIF atlas,[25] expanded to include white matter and brought into the native space of individuals with epilepsy. When surgical individuals were analyzed together with non-surgical individuals, the lobe including the surgical resection was defined as *lobe mask* (for the analysis of surgical individuals only, *resection masks* were used). For non-surgical individuals with epilepsy the pSOZ was extracted from patient records and determined by a team of 3 expert physicians with over 20 years of experience based on the results of a multimodal diagnostic work-up as part of the clinical routine.[26] The diagnostic work-up included MRI, video-EEG, neuropsychological assessment, and SPECT for all individuals, as well as PET (8 individuals) and stereotactic EEG (11 individuals) for a subset. The expert physicians were blinded to the identities of the individuals and to the SPECT findings. We assessed the cross-rater agreement between the pSOZ and the 3 raters using Fleiss' Kappa.[27]

Quantitative Evaluation. We quantitatively evaluated the ictal SPECT image analysis of each pipeline (IISASL, ISASL, and ISAS) with the Dice score (1) and the mean Euclidean distance (2):

1. The Dice score quantifies the overlap of hyperperfusion (H) and the ground truth (G).[28]

$$\text{Dice} = \frac{2|H \cap G|}{|H| + |G|} \quad (1)$$

2. The mean Euclidean distance between the Centers of Gravity of hyperperfusion clusters from the center of gravity of the ground truth (see Fig. 2 for a schematic illustrating Dice score and Euclidean distance). Permutation-based non-parametric testing and TFCE has never been applied to ASL and ictal SPECT imaging, nor have metrics such as the Dice score or the mean Euclidean distance been determined. For this reason, we had to determine the optimal threshold for the output of each pipeline, by calculating the mean Dice score for thresholds of $p = (0, 0.2, 0.3, 0.4, 0.5, 0.6, 0.7, 0.8, 0.85, 0.9, 0.95, 0.99, 0.999, 0.9999, 0.99999, 0.999999)$. The threshold with the maximum Dice score was used for all further analyses. Both metrics were calculated for each pipeline (IISASL, ISASL, and ISAS). Metrics were all calculated using *Nibabel* (version 4.0, https://nipy.org/nibabel/).[29,30]

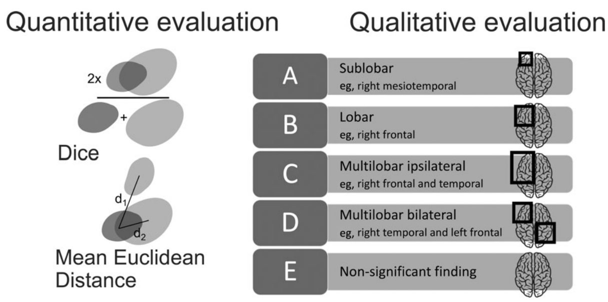

FIGURE 2: Schematic overview of quantitative and qualitative evaluation.

All hyperperfusion clusters above the chosen threshold contributed to the Dice score calculation, therefore including those of possible remote activation patterns. To assess the impact of remote activation patterns, we also evaluated the Dice score of the sole hyperperfusion cluster with the highest overlap with the ground truth. Lastly, we assessed the effect of seizure outcome on the above-mentioned Dice score and mean Euclidean distance. We split the cohort into 2 groups based on the Engel outcome at last clinical follow-up; Group 1 included seizure-free individuals (Engel I). Group 2 was not seizure-free following surgery (Engel II, III, and IV). We compared the Dice score and mean Euclidean distance between the 2 groups for each pipeline (ISAS, IISASL and ISASL) by means of an unpaired 2-sided t-test.

Qualitative Evaluation. Based on the alignment between the ictal SPECT output and the ground truth, we qualitatively classified the output of all 3 pipelines into categories adapted from El Tahry and colleagues.[31] Category A includes findings aligned on a sublobar level, Category B on a lobar level, and Category C on a hemispheric level. Category D contains findings in multiple regions on both hemispheres, and Category E describes null-result findings (see Fig. 2 for a schematic visualization). Results in categories A and B are considered localizing. Results in categories C, D, and E are considered non-localizing. In contrast to a purely qualitative visual categorization by raters as conducted before, in this study, we have quantified and automatized the categorization: For category A the overlap of hyperperfusion and ground truth with GIF-atlas-based[25,32] parcellations of the brain was determined. For categories B and C, these parcellations were grouped into lobar regions and hemispheres, respectively. We compared these overlaps by means of the cosine distance measure using *SciPy* (version 1.9, https://docs.scipy.org),[33] producing a cosine difference for each category A to D.

Results

Study Group

Surgical Individuals. A total of 43 individuals with epilepsy underwent surgery and met our inclusion criteria (mean age at presurgical evaluation: 31.9 ± 11.95 years; 17 female [40%]). 23/43 had focal cortical dysplasia (FCD), 7/43 had hippocampal sclerosis, and the remaining 13/43 had tumors, heterotopia, or other focal pathologies. Anatomical locations of focal pathologies were: 22/43 frontal, 15/43 temporal, 2/43 parietal, 2/43 parieto-occipital, and 2/43 occipital. Surgical outcome at the last follow-up (on average 3.9 years after surgery) was: 30/43 Engel I, 5/43 Engel II, 4/43 Engel III, and 4/43 Engel IV. Further demographical data can be found in Table S3.

Non-surgical Individuals. A total of 73 individuals with epilepsy underwent SPECT imaging and met our inclusion criteria, but declined or were not admitted to surgery (mean age: 31.1 ± 9.5 years; 32 female [44%]). The lobe containing the pSOZ was; 36/73 temporal, 32/73 frontal, 6/73 parietal, 3/73 occipital and 2/73 insular (note for 6 individuals the pSOZ was multilobal). Further demographical data can be found in Table S4. We separately assessed the pSOZ-rater-agreement for *hemisphere* (left, right, bilateral) and *lobe* (frontal, temporal, occipital, insular and parietal) of the non-surgical individuals. The Fleiss' Kappa for the hemisphere ratings was $\kappa = 0.761$ ($p < 0.001$) and $\kappa = 0.692$ ($p < 0.001$) for the lobar rating. Both scores indicate substantial interrater agreement, which is generally considered for Kappa scores of 0.61–0.80.[34]

Group Tests between SPECT and ASL Scan-to-Scan Differences

We found no significant (FWE-corrected $p < 0.05$) differences between the histogram-matched scan-to-scan variations of the healthy ASL and SPECT controls in any region of the brain.

Evaluation of Surgical Individuals

Quantitative Evaluation. First, we evaluated the output of each pipeline (IISASL, ISASL, and ISAS) quantitatively for all individuals who underwent epilepsy surgery (n = 43). We found that the mean Dice score for IISASL was significantly higher (paired t-tests, $P < 0.05$) than for ISAS with the affected lobe as the ground truth (see Table 1 and Fig. 3). The mean Euclidean distance was significantly lower in IISASL and ISASL compared to ISAS (paired *t*-tests, $p < 0.001$). The effect size (Cohen's d) was *moderate* (0.5–1.0) to *strong* (>1.0) in both cases respectively.[35,36] Additional metrics (true positive rate and positive predictive value) are reported in Table S5.

Qualitative Evaluation. We then qualitatively evaluated each pipeline by categorizing the output for each surgical individual as localizing (categories A and B) or non-localizing (categories C, D, and E) based on the cosine distance. We determined a cosine distance threshold of 0.6, 0.55, 0.1, and 1 for categories A, B, C, and D, respectively. The average cosine distances for each pipeline can be found in the supplement (Table S6). IISASL generated localizing results (categories A and B) in 26/43 [60%] individuals, while ISAS generated 21/43 [49%]

TABLE 1. Quantitative Results for Each Pipeline

Ground Truth/ Cohort	Surgical Outcome	Metric	ISAS	IISASL$^{vs. ISAS}$	ISASL$^{vs. ISAS}$
Resection masks/ surgical individuals (n = 43)	Seizure-free (Engel I), n = 30	Dice score, mean ± SD	0.074 ± 0.10	0.093 ± 0.12	0.085 ± 0.12
		Mean Euclidean distance, mean ± SD, mm	68.5 ± 18.3	**47.7 ± 24.3*****	**43.5 ± 21.9******
	Non-seizure-free (Engel II, III, IV), n = 13	Dice score, mean ± SD	0.039 ± 0.080	0.04 ± 0.045	0.057 ± 0.082
		Mean Euclidean distance, mean ± SD	71.2 ± 17.2	68.4 ± 20.3	**52.6 ± 26.4***
LOBE MASKS/ surgical individuals (n = 43)	Seizure-free (Engel I), n = 30	Dice score, mean ± SD	0.142 ± 0.129	**0.220 ± 0.178*****	0.200 ± 0.181
		Mean Euclidean distance, mean ± SD, mm	72.7 ± 14.3	**51.7 ± 22.6******	**42.6 ± 26.3******
	Non-seizure-free (Engel II, III, IV), n = 13	Dice score, mean ± SD	0.078 ± 0.087	0.147 ± 0.152	0.140 ± 0.155
		Mean Euclidean distance, mean ± SD	77.7 ± 17.6	70.9 ± 21.1	**54.3 ± 28.7***
LOBE MASKS/non-surgical individuals (n = 73)		Dice score, mean ± SD	0.124 ± 0.132	**0.216 ± 0.148******	**0.157 ± 0.146****
		Mean Euclidean distance, mean ± SD, mm	68.4 ± 16.6	**52.6 ± 21.4******	**54.6 ± 23.6******

Note: The table shows the quantitative results (Dice and mean Euclidean distance) for ISAS, IISASL, and **ISASL for surgical individuals (top) and non-surgical individuals** (bottom). For consistency, results of the evaluation calculated with *lobe masks* for both groups are displayed. The results of the surgical individuals are subdivided into individuals with Engel I outcome (seizure freedom) versus Engel II, III and IV outcome (non-seizure-free). A paired t-test was performed between ISAS and IISASL as well as ISAS and ISASL. Significant ($p < 0.05$) differences are bold.
*$p < 0.05$.
**$p < 0.001$.
***$p < 0.0001$.
****$p < 0.00001$.

localizing results. ISASL yielded 22/43 [51%] localizing results (see Table 2 and Fig. 3). Hence, IISASL generated the most localizing results, followed by ISASL and ISAS, though the differences did not reach statistical significance (chi-squared tests $p > 0.05$).

Evaluation and Post-Surgical Outcome. Furthermore, we investigated differences in the qualitative and quantitative outcomes of the surgical individuals, based on their post-surgery Engel outcome by dividing the cohort into 2 groups; seizure-free (Engel I) with n = 30 individuals, and non-seizure-free (Engel II, III, and IV) with n = 13 individuals. Dice scores were higher and the mean Euclidean distance to the ground truth was lower for the seizure-free group compared to the non-seizure-free group (see Fig. 4 and Table S7) for all pipelines. However, the only statistically significant (unpaired t-test, $p = 0.01$) difference was found comparing the mean Euclidean distance of the seizure-free and non-seizure-free group for the IISASL pipelines. Qualitative evaluation corroborated findings of the quantitative evaluation: For the seizure-free group, ISAS yielded localizing results (categories A and B)

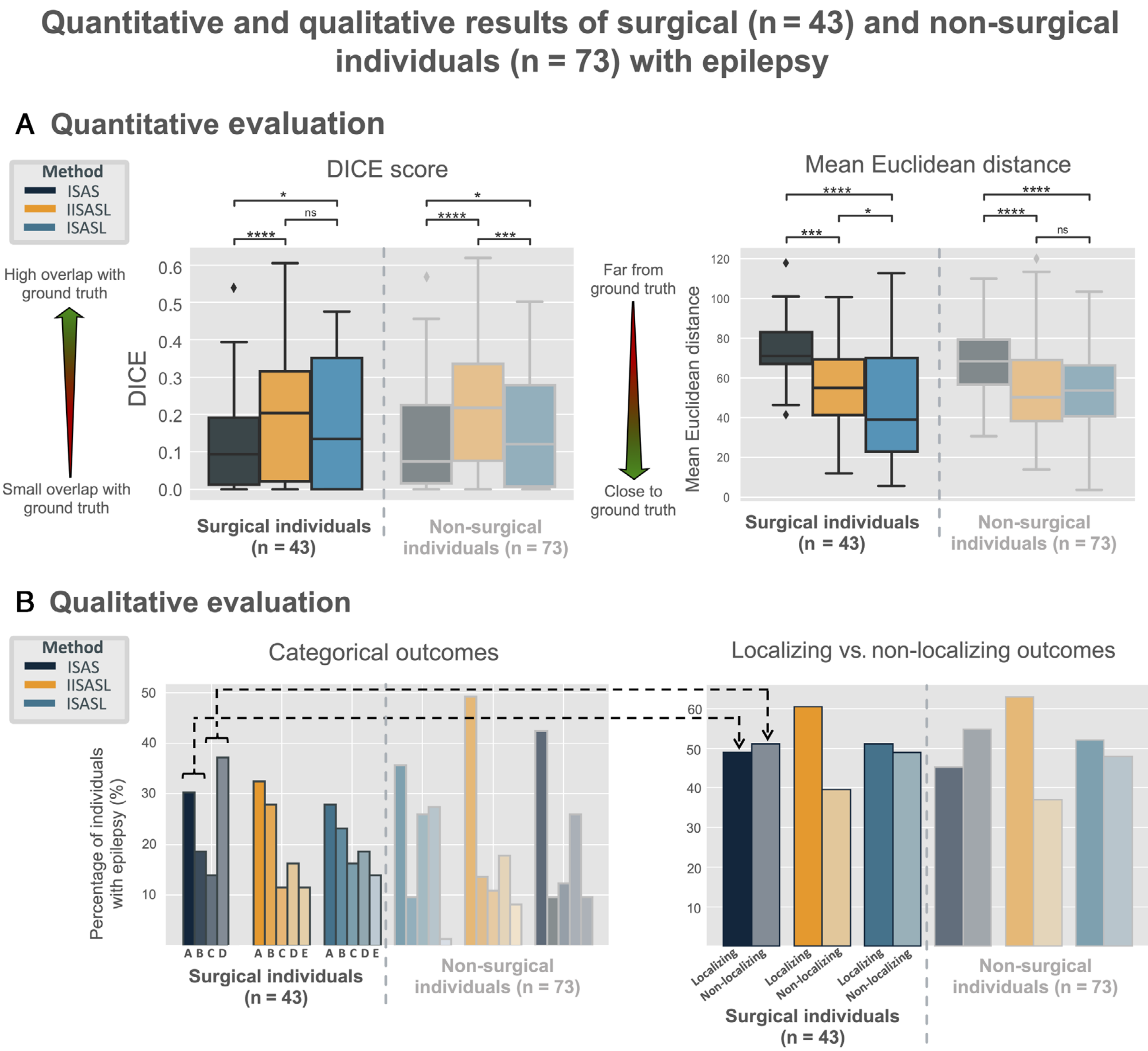

FIGURE 3: Quantitative and qualitative evaluation of pipeline results in surgical (left) and non-surgical (right) individuals with epilepsy. (A) Results of the Dice score and mean Euclidean distance of ISAS, IISASL, and ISASL are shown. The lobe containing the presumed seizure onset zone is defined as the ground truth (*lobe masks* for consistency between surgical and non-surgical individuals). Paired *t*-test between each method and ISAS were performed, where * represents a significant difference of $p < 0.05$, **: $p < 0.001$, ***: $p < 0.0001$, ****: $p < 0.00001$, ns: non-significant. (B) Qualitative evaluations of ISAS, IISASL, and ISASL is presented. Outcomes A and B are considered localizing, as visualized by the arrows. ASL, Arterial Spin Labeling; ISAS, Interictal SPECT Analysis by SPM; IISASL, Ictal-interictal SPECT-ASL; ISASL, ictal SPECT-ASL.

in 18/30 cases (60%), IISASL yielded 20/30 (67%) localizing results, whilst ISASL yielded 15/30 (50%) localizing results; however, the differences between all 3 pipelines were non-significant (chi-squared tests $p > 0.05$).

In summary, among surgical individuals with epilepsy, IISASL yielded the best results across both quantitative (Dice and mean Euclidean distance) and qualitative (localizing versus non-localizing) measures, followed by ISASL and ISAS. For all pipelines, quantitative and qualitative metrics were better in the seizure-free group, though the only significant differences were found for IISASL.

Please see results of IISASL and ISASL for 3 representative individuals in Figure 5. Results on a case-wise level for all surgical individuals including Engel outcome are provided in the supplement (Table S3).

Evaluation of Non-surgical Individuals

Additionally, we evaluated the non-surgical individuals with epilepsy both quantitatively (Dice score and mean Euclidean distance) and qualitatively (localizing vs. non-localizing).

TABLE 2. Qualitative Results for Each Pipeline

Parameter	Category	ISAS, Number (%)	IISASL, Number (%)	ISASL, Number (%)
Seizure-free (Engel 1), n = 30, *resection masks* as ground truth	A	10 (33%)	10 (33%)	8 (27%)
	B	8 (27%)	10 (33%)	7 (23%)
	C	2 (7%)	4 (13%)	7 (23%)
	D	10 (33%)	5 (17%)	3 (10%)
	E	0	1 (3%)	5 (17%)
Non-seizure-free (Engel II, III, Engel IV), n = 13, *resection masks* as ground truth	A	3 (23%)	4 (31%)	4 (31%)
	B	0	2 (15%)	3 (23%)
	C	4 (31%)	1 (8%)	0 (0%)
	D	6 (46%)	5 (38%)	5 (39%)
	E	0	1 (8%)	1 (8%)
Non-Surgical Individuals, *LOBE masks* as ground truth	A	26 (35.6%)	36 (49.3%)	31 (42.5%)
	B	7 (9.6%)	10 (13.7%)	7 (9.6%)
	C	19 (26%)	8 (11.0%)	9 (12.3%)
	D	20 (27.4%)	13 (17.8%)	19 (26%)
	E	1 (1.4%)	6 (8.2%)	7 (9.6%)

Note: The table shows the qualitative results for ISAS, IISASL, and ISASL for surgical individuals (top) and non-surgical individuals (bottom). The results of the surgical individuals is subdivided into individuals with Engel I outcome (seizure freedom) versus Engel II, III and IV outcome (non-seizure-free).
Abbreviations: ISAS, interictal SPECT analysis by SPM; IISASL, ictal-interictal SPECT-ASL; ISASL, ictal SPECT-ASL.

Quantitative Evaluation. As in the cohort of surgical individuals, the mean Dice score for IISASL was significantly higher (paired t-tests, $p < 0.05$) than for ISAS (see Fig. 3) and the mean Euclidean distance was significantly lower in IISASL and ISASL compared to ISAS (paired *t*-tests, $p < 0.001$). Additional metrics (true positive rate and positive predictive value) are reported in Table S5.

Qualitative Evaluation. IISASL generated 46/73 [63%] localizing results, compared to 33/73 (45%) for ISAS and 38/73 (52%) for ISASL. In contrast to the surgical individuals, the differences between IISASL and ISAS were statistically significant (chi-squared tests $p < 0.05$).

Results on a case-wise level for all non-surgical individuals are provided in the supplement (Table S4).

Combined Evaluation of Surgical and Non-surgical Individuals

To get a comprehensive picture of the entire cohort of individuals with epilepsy, we combined the cohorts of surgical and non-surgical individuals. By defining the affected lobe as the ground truth, we were able to combine the quantitative and qualitative results of both groups. As in the surgical individuals with epilepsy alone, in the combined group of surgical and non-surgical individuals IISASL yielded the best results across both quantitative and qualitative measures, followed by ISASL and ISAS, respectively. Localizing results for the combined group were 72/116 for IISASL [62%] 54/116 [47%] for ISAS and 60/116 [52%] for ISASL. In summary, as with the surgical individuals, the combined evaluation of surgical and non-surgical individuals showed that IISASL yielded the best results across both quantitative and qualitative measures followed by ISASL and ISAS.

Evaluation of the Framework

Finally, we investigated how many individuals can potentially be spared the interictal SPECT image and how the 2 pipelines IISASL and ISASL can be combined into a clinical workflow. As described above, 26 of the 43 surgical individuals had localizing results in the qualitative evaluation of IISASL. Of those 26 individuals, ISASL yielded localizing results in 16 cases. Out of the 46 of the 73 non-surgical individuals with localizing results in

FIGURE 4: Quantitative and qualitative results for seizure-free and non-seizure-free surgical outcomes. (A) The mean Dice score and mean Euclidean distance for the group of individuals with a seizure-free (Engel I) post-operative outcome (n = 30) and non-seizure-free (Engel II, III, and IV) post-operative outcomes (n = 13). Unpaired *t*-tests between the 2 groups (seizure-free vs. non-seizure-free) were performed, where * represents a significant difference of $p < 0.05$, **: $p < 0.001$, ***: $p < 0.0001$, ****: $p < 0.00001$, ns: non-significant. (B) Qualitative evaluations of ISAS, IISASL, and ISASL is presented for seizure free (Engel I) versus non-seizure free outcomes (Engel II, III, IV). Outcomes A and B are considered localizing. ASL, arterial spin labeling; ISAS, interictal SPECT analysis by SPM; IISASL, ictal-interictal SPECT-ASL; ISASL, ictal SPECT-ASL.

IISASL, ISASL yielded localizing results in 31 cases. Hence, overall, in 47/72 cases [65%], the ictal image would have been sufficient (and the interictal acquisition could have been omitted, see Fig. 6A). The high overlap coefficient (0.78) between the individuals with localizing IISASL and ISASL results reflects the similarity between the 2 groups. The combination of both pipelines (either localizing ISASL or localizing IISASL) yields localizing results in 85/116 [73%] cases. In contrast, ISAS yields localizing results in 54/116 [47%] cases. The combination of IISASL and ISASL is, thus, 26% better than the current gold standard ISAS in the qualitative evaluation.

Threshold and Cluster Analysis

All above-mentioned calculations were performed at an optimal threshold for each pipeline, which we determined by maximizing the average Dice score across the surgical cohort. We found the highest average Dice score for the ISAS pipeline to be at a height threshold of $p = 10^{-4}$ (FWE-corrected). For the IISASL pipeline, the highest average Dice score was at a threshold of $p = 0.6$ and for the ISASL at $p = 0.95$ (FWE-corrected and with TFCE). The threshold as a function of the Dice score is visualized in Figure S8. In the separate analysis of the cluster with the highest overlap with the ground truth we observed that IISASL reached the highest Dice scores, followed by ISASL and then ISAS. Additionally, we found no significant difference between the Dice scores derived from considering all hyperperfusion clusters versus solely the hyperperfusion cluster with the highest overlap with the ground truth for both IISASL and ISASL (paired t-test, $p > 0.05$, see Figure S9).

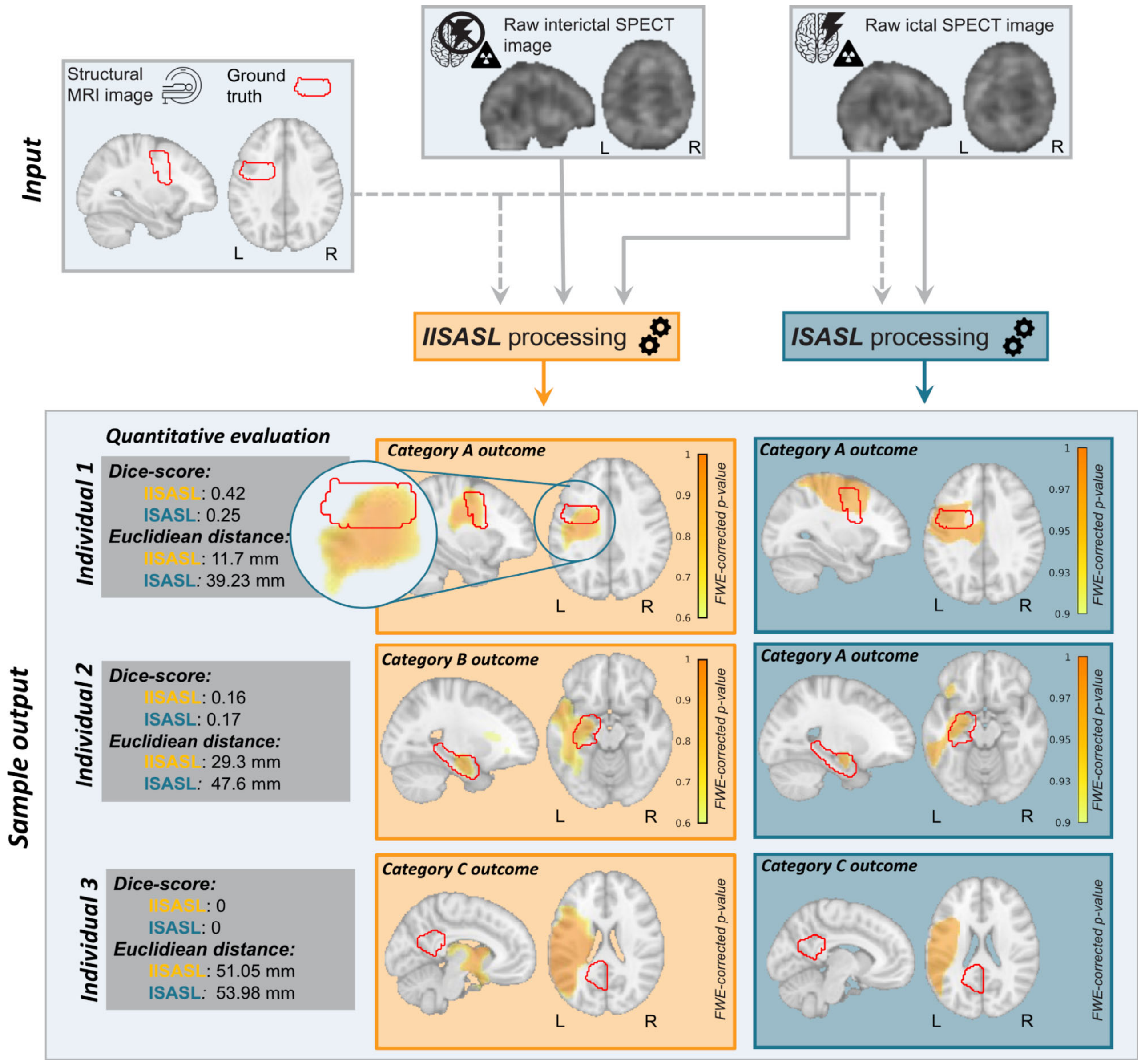

FIGURE 5: Exemplary results of IISASL and ISASL analysis for 3 individuals who underwent epilepsy surgery in relation to the respective ground truth. Individual 1 was diagnosed with a left frontal focal cortical dysplasia, individual 2 was diagnosed with left temporal hippocampal sclerosis, individual 3 was diagnosed with left parieto-occipital ganglioglioma. The ground truth (red) was drawn manually based on the surgical resection (*resection masks*). All 3 individuals had an Engel I post-surgical outcome.

Discussion

We systematically evaluated ISAS, the current gold standard analysis of ictal SPECT, by means of quantitative (Dice score, Euclidean distance) and qualitative measures in a cohort of 43 individuals with epilepsy who underwent epilepsy surgery and of 73 individuals with epilepsy who did not undergo surgery. We developed 2 pipelines, integrating an ASL controls cohort and using non-parametric permutation testing: One with the ictal and interictal SPECT image (IISASL) and 1 with the ictal SPECT image only (ISASL). When applying quantitative and qualitative measures to IISASL and ISASL and comparing it to ISAS, both pipelines showed relevantly better results. In surgical individuals, ISASL also led to better results in the seizure-free group than in the non-seizure-free group. We propose a novel protocol for the acquisition and analysis of ictal SPECT data below, maximizing its diagnostic importance and minimizing radiation exposure.

Subgroup Analyses

We divided our cohort of individuals with epilepsy into surgical and non-surgical individuals and further divided

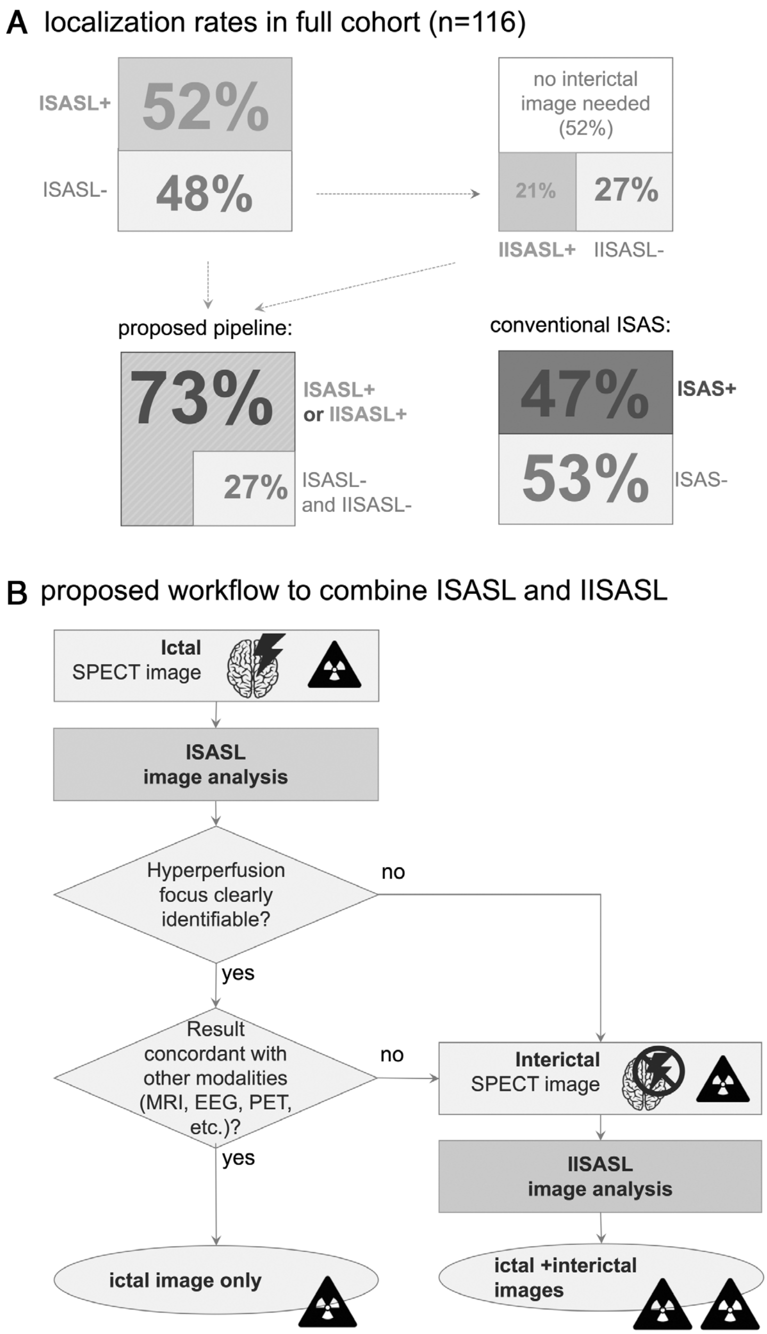

FIGURE 6: Novel SPECT protocol proposed. For 52% of individuals with epilepsy localizing results could be achieved with just the ictal SPECT image (ISASL) compared to 64% when ictal and interictal images are included in the analysis (IISASL). By combining the 2 methods in the recommended workflow, for 73% of individuals with epilepsy localizing results can be achieved. ISAS, the previous gold-standard analysis yields localizing results in only 47% of the cases. ISAS, interictal SPECT analysis by SPM; IISASL, ictal-interictal SPECT-ASL; ISASL, ictal SPECT-ASL; FWE-corrected, family-wise error corrected.

the group of surgical individuals into seizure-free and non-seizure-free following surgery. For the non-surgical individuals, we found substantial interrater agreement regarding the pSOZ (Fleiss' Kappa 0.761 and 0.692 for hemisphere and lobe, respectively) despite the raters being blinded to identity of the individuals and to the respective SPECT findings. Furthermore, there were no significant differences between the qualitative results between surgical and non-surgical cohorts. Nevertheless, the pSOZ can be defined to a much greater degree of certainty for the surgical individuals as ground truth (especially for the Engel I group), motivating this subdivision of our cohort and separate reporting of all results for surgical and non-surgical individuals. The comparison of seizure-free vs. non-seizure-free surgical individuals revealed worse quantitative results for the non-seizure-free group for all pipelines (see Table 1 and Fig. 4). This difference was only significant for the mean Euclidean distance for IISASL, suggesting a greater selectivity of IISASL.

Metrics for Evaluation

Compared to lesion detection and segmentation of MRI images, Dice scores in our study are generally low and show high variance. This reflects that although ictal SPECT can help identify the location of the seizure focus, accurate segmentation of a potentially epileptogenic lesion cannot be expected from this modality. Dice scores were generally higher when calculated with the *lobe mask* as compared to the *resection mask*, since *resection masks* are on average 14.2 times smaller than *lobe masks* (except for the case of lobectomy). For this reason, we present a comprehensive array of metrics, including the mean Euclidean distance, qualitative categories based on the cosine distance as well as the positive predictive value, and the true positive rate provided in the supplement (please see Tables S5 and S6).

Epileptic Networks

Further potential reasons for non-perfect alignment of hyperperfusion and ground truth are the low resolution of SPECT, the spread of ictal activity, and the nature of ictal hyperperfusion, which is not limited to the seizure onset zone.[37,38] Through spread of epileptic activity and resulting hyperperfusion, epileptic networks can be revealed and studied by ictal SPECT.[39,40] Although not the focus of this study, it is important to consider the potential impact of epileptic networks on our results. We found no significant difference between Dice scores of the cluster with the highest overlap with the ground truth and Dice scores of all hyperperfusion clusters for IISASL and ISASL. This does not mean that the role of remote activation in epileptogenic networks is irrelevant, but may indicate that significant hyperperfusion is often focused on 1 anatomical area. The question how well ictal SPECT findings can be understood by network models, however, depends on several factors including the injection timing, location of the SOZ and types of seizures.[40–44] Advanced modelling including analysis of structural and functional connectivity would be needed to for the analysis of epileptic networks using SPECT and is subject to future research.

Limitations of the Study

We assessed the utility of the IISASL and ISASL pipeline in a retrospective dataset of individuals who underwent ictal SPECT imaging at our center. Our study is limited in that we have not prospectively evaluated the utility of our pipelines, nor did we prospectively assess our proposed workflow (Fig. 6) clinically. Furthermore, we categorized findings as localizing vs. non-localizing based on the cosine similarity between the output of the pipelines and the ground truth. Whilst we consider the quantitative categorization advantageous, a human rater assessment may be more similar to the clinical real-world scenario and help to establish the clinical utility of the pipelines. The many potential biases of ictal SPECT processing include latency between seizure onset and tracer injection as well as the heterogeneous types of pathologies in the cohort of individuals with epilepsy.[2,45,46] Finally, we did not analyze hypoperfusion in this study, which may play a role especially in the context of epileptic networks.[43]

Proposed New Protocol for Acquisition and Analysis of Ictal SPECT

Differences between the outcomes of ISASL and IISASL may be explained by interictal hypoperfusion, which needs to be analyzed only in a minority of cases to reveal relative ictal hyperperfusion.[5,47] The acquisition of interictal ASL images may be helpful to identify these cases or further enhance processing in the future. Here, we propose to use our open-source code and the ASL healthy controls data for analysis of the ictal SPECT image before acquisition of the interictal one and proceed with the acquisition of the interictal image only in cases with negative or inconclusive results. See Figure 6B for a schematic of this protocol. As such, the results of the ISASL analysis must be considered in relation to other modalities in the presurgical work-up and in cases of discrepancy, an interictal SPECT image must be acquired. Hence, fewer people will undergo ictal SPECT imaging without additional diagnostic benefit and many individuals can be spared half the radiation dose.

Clinical Value

Ictal SPECT is an expensive and time-consuming investigation, in which individuals are exposed to an average radiation dose of 6.8 millisievert, which is equivalent to the radiation dose from over 4 conventional head CT scans.[48] However, it is also unique in the presurgical workup of individuals with epilepsy. It is the only imaging modality geared towards visualizing correlates of an epileptic seizure, while the rest of epilepsy imaging is centered around the potentially epileptogenic lesion. Both IISASL AND ISASL localize the SOZ more accurately, potentially increasing the number of individuals with epilepsy who are candidates for epilepsy surgery; especially those with otherwise inconclusive results and individuals with nonlesional MRI findings.[49] In these cases, ictal SPET may aid in the development of pre-implantation (Stereo-EEG)-hypotheses. Furthermore, the proposed new protocol including the application of ISASL only may save half the radiation dose of conventional ictal-interictal SPECT methods, while conserving clinical and economic resources.

Acknowledgements

F.B. received funding from the BONFOR research commission (Grant 2021-4-05) of the medical faculty of the University of Bonn. Open Access funding enabled and organized by Projekt DEAL.

Author Contributions

F.B., L.W., T.Bauer., M.S., and T.R. contributed to the conception and design of the study; F.B., L.W., T.Bauer., and T.R. prepared the text and figures. All authors contributed to data acquisition and analysis.

Data Availability Statement

The code for IISASL and ISASL and ASL scan-to-scan differences can be found at https://www.github.com/fbitzer/ictal-SPECT-ASL. The data that support the findings of this study are available on request from the corresponding author. The data of individuals with epilepsy are not publicly available as they contain information that could compromise the privacy of participants.

Potential Conflict of Interest

Nothing to declare.

References

1. Fiest KM, Sauro KM, Wiebe S, et al. Prevalence and incidence of epilepsy. Neurology 2017;88:296–303. https://doi.org/10.1212/WNL.0000000000003509.
2. von Oertzen TJ. PET and ictal SPECT can be helpful for localizing epileptic foci. Curr Opin Neurol 2018;31:184–191.
3. Rowe CC, Berkovic SF, Sia STB, et al. Localization of epileptic foci with postictal single photon emission computed tomography. Ann Neurol 1989;26:660–668.
4. Hougaard K, Oikawa T, Sveinsdottir E, et al. Regional cerebral blood flow in focal cortical epilepsy. Arch Neurol 1976;33:527–535.
5. Chang DJ, Zubal IG, Gottschalk C, et al. Comparison of statistical parametric mapping and SPECT difference imaging in patients with temporal lobe epilepsy. Epilepsia 2002;43:68–74.
6. Kazemi NJ, Worrell GA, Stead SM, et al. Ictal SPECT statistical parametric mapping in temporal lobe epilepsy surgery. Neurology 2010;74:70–76.
7. Sulc V, Stykel S, Hanson DP, et al. Statistical SPECT processing in MRI-negative epilepsy surgery. Neurology 2014;82:932–939.
8. Taha AA, Hanbury A. Metrics for evaluating 3D medical image segmentation: analysis, selection, and tool. BMC Med Imaging 2015;15:29.
9. McNally KA, Paige ALB, Varghese G, et al. Localizing value of ictal-interictal SPECT analyzed by SPM (ISAS). Epilepsia 2005;46:1450–1464.
10. Eklund A, Nichols TE, Knutsson H. Cluster failure: why fMRI inferences for spatial extent have inflated false-positive rates. Proc Natl Acad Sci U S A 2016;113:E4929.
11. Nichols T, Holmes A. Nonparametric permutation tests for functional neuroimaging. In: *Human brain function*. 2004:887–910. https://doi.org/10.1016/B978-012264841-0/50048-2.
12. Alsop DC, Detre JA, Golay X, et al. Recommended implementation of arterial spin-labeled perfusion MRI for clinical applications: a consensus of the ISMRM perfusion study group and the European consortium for ASL in dementia. Magn Reson Med 2015;73:102–116.
13. Schidlowski M, Stirnberg R, Stöcker T, Rüber T. Reliability of quantitative transverse relaxation time mapping with T2-prepared whole brain pCASL. Sci Rep 2020;10:18299.
14. Neumann K, Schidlowski M, Günther M, et al. Reliability and reproducibility of Hadamard encoded pseudo-continuous arterial spin labeling in healthy elderly. Front Neurosci 2021;15:711898. https://doi.org/10.3389/fnins.2021.711898.
15. Engel J. Update on surgical treatment of the epilepsies. Neurology 1993;43:1612.
16. Buxton RB, Frank LR, Wong EC, et al. A general kinetic model for quantitative perfusion imaging with arterial spin labeling. Magn Reson Med 1998;40:383–396.
17. Chappell MA, Groves AR, Whitcher B, Woolrich MW. Variational Bayesian inference for a nonlinear forward model. IEEE Trans Signal Process 2009;57:223–236.
18. Winkler AM, Ridgway GR, Webster MA, et al. Permutation inference for the general linear model. Neuroimage 2014;92:381–397.
19. Scheinost D, Teisseyre TZ, Distasio M, et al. New open-source ictal SPECT analysis method implemented in BioImage suite. Epilepsia 2010;51:703–707.
20. Jenkinson M, Beckmann CF, Behrens TEJ, et al. FSL. Neuroimage 2012;62:782–790.
21. Henschel L, Conjeti S, Estrada S, et al. FastSurfer-a fast and accurate deep learning based neuroimaging pipeline. Neuroimage 2020;219:117012.
22. Dale AM, Fischl B, Sereno MI. Cortical surface-based analysis: I segmentation and surface reconstruction. Neuroimage 1999;9:179–194.
23. van der Walt S, Schönberger JL, Nunez-Iglesias J, et al. Scikit-image: image processing in python. PeerJ 2014;2:e453.
24. Fischl B, Salat DH, Busa E, et al. Whole brain segmentation: automated labeling of neuroanatomical structures in the human brain. Neuron 2002;33:341–355.
25. Cardoso MJ, Modat M, Wolz R, et al. Geodesic information flows: spatially-variant graphs and their application to segmentation and fusion. IEEE Trans Med Imaging 2015;34:1976–1988.
26. Schulte F, Bitzer F, Gärtner FC, et al. The diagnostic value of ictal SPECT—A retrospective, semiquantitative monocenter study. Epilepsia Open 2023;8:183–192. https://doi.org/10.1002/epi4.12694.
27. Fleiss JL. Measuring nominal scale agreement among many raters. Psychol Bull 1971;76:378–382.
28. Dice LR. Measures of the amount of ecologic association between species. Ecology 1945;26:297–302.
29. Brett M, Markiewicz CJ, Hanke M, et al. nipy/nibabel: (4.0.0). Zenodo 2022. https://doi.org/10.5281/zenodo.6658382.
30. Gorgolewski K, Burns CD, Madison C, et al. Nipype: a flexible, lightweight and extensible neuroimaging data processing framework in python. Front Neuroinform 2011;5. https://www.frontiersin.org/journals/neuroinformatics/articles/10.3389/fninf.2011.00013.
31. el Tahry R, Wang ZI, Thandar A, et al. Magnetoencephalography and ictal SPECT in patients with failed epilepsy surgery. Clin Neurophysiol 2018;129:1651–1657.

32. Alim-Marvasti A, Romagnoli G, Dahele K, et al. Probabilistic landscape of seizure semiology localizing values. Brain Commun 2022;4: fcac130.

33. Gommers R, Oliphant TE, Haberland M, et al. SciPy 1.0: fundamental algorithms for scientific computing in Python. Nat Methods 2020;17: 261–272.

34. Landis JR, Koch GG. The measurement of observer agreement for categorical data. Biometrics 1977;33:159–174.

35. Cohen J. *Statistical power analysis for the behavioral sciences*. 2nd ed. Lawrence Erlbaum Associates Publishers, 1988.

36. Cohen L, Manion L, Morrison K. *Research methods in education*. Routledge, 2007.

37. la Fougère C, Rominger A, Förster S, et al. PET and SPECT in epilepsy: a critical review. Epilepsy Behav 2009;15:50–55. https://doi.org/10.1016/j.yebeh.2009.02.025.

38. Van Paesschen W, Dupont P, Sunaert S, et al. The use of SPECT and PET in routine clinical practice in epilepsy. Curr Opin Neurol 2007; 20:194–202.

39. Wichert-Ana L, Velasco TR, Terra-Bustamante VC, et al. Typical and atypical perfusion patterns in periictal SPECT of patients with unilateral temporal lobe epilepsy. Epilepsia 2001;42:660–666.

40. Kheder A, Thome U, Aung T, et al. Investigation of networks underlying hyperkinetic seizures utilizing ictal SPECT. Neurology 2020;95: e637–e642.

41. Krishnan B, Tousseyn S, Nayak CS, et al. Neurovascular networks in epilepsy: correlating ictal blood perfusion with intracranial electrophysiology. Neuroimage 2021;231:117838.

42. Ho SS, Berkovic SF, McKay WJ, et al. Temporal lobe epilepsy subtypes: differential patterns of cerebral perfusion on ictal SPECT. Epilepsia 1996;37:788–795.

43. Krishnan B, Tousseyn S, Wang ZI, et al. Novel noninvasive identification of patient-specific epileptic networks in focal epilepsies: linking single-photon emission computed tomography perfusion during seizures with resting-state magnetoencephalography dynamics. Hum Brain Mapp 2023;44:1695–1710.

44. Shin WC, Hong SB, Tae WS, Kim SE. Ictal hyperperfusion patterns according to the progression of temporal lobe seizures. Neurology 2002;58:373–380.

45. Ramchuankiat S, Jarumaneeroj P, Limotai C, et al. Impact of injection time on migration of SPECT seizure onset in temporal lobe epilepsy. 2017 39th Annu Int Conf IEEE Eng Med Biol Soc 2017;1465–1468. https://ieeexplore.ieee.org/document/8037111.

46. Stamoulis C, Verma N, Kaulas H, et al. The promise of subtraction ictal SPECT co-registered to MRI for improved seizure localization in pediatric epilepsies: affecting factors and relationship to the surgical outcome. Epilepsy Res 2017;129:59–66.

47. Lee JD, Kim HJ, Lee BI, et al. Evaluation of ictal brain SPET using statistical parametric mapping in temporal lobe epilepsy. Eur J Nucl Med 2000;27:1658–1665.

48. Holman BL, Johnson KA, Gerada B, et al. The Scintigraphic appearance of Alzheimer's disease: a prospective study using technetium-99m-HMPAO SPECT. J Nucl Med 1992;33:181–185.

49. von Oertzen TJ, Gröppel G, Katletz S, et al. SPECT and PET in nonlesional epilepsy. Clinical Epileptology 2023;36:104–110. https://doi.org/10.1007/s10309-023-00577-1.